Published in final edited form as:
Biomaterials. 2012 August ; 33(23): 5723–5731. doi:10.1016/j.biomaterials.2012.04.042.

Tissue engineering the monosynaptic circuit of the stretch reflex arc with co-culture of embryonic motoneurons and proprioceptive sensory neurons

Xiufang Guo[a,1], **Jennifer E. Ayala**[a,1], **Mercedes Gonzalez**[a], **Maria Stancescu**[a,b], **Stephen Lambert**[a,c], and **James J. Hickman**[a,b,*]

[a]Hybrid Systems Lab, NanoScience Technology Center, University of Central Florida, 12424 Research Parkway, Suite 400, Orlando, FL 32826, USA

[b]Department of Chemistry, 4000 Central Florida Blvd., Physical Sciences Building (PS) Room 255, University of Central Florida, Orlando, FL 32816-2366, USA

[c]College of Medicine, University of Central Florida, 12201 Research Parkway, Suite 479, Room 463, Orlando, FL 32826, USA

Abstract

The sensory circuit of the stretch reflex arc is composed of intrafusal muscle fibers and their innervating proprioceptive neurons that convert mechanical information regarding muscle length and tension into action potentials that synapse onto the homonymous motoneurons in the ventral spinal cord which innervate the extrafusal fibers of the same muscle. To date, the in vitro synaptic connection between proprioceptive sensory neurons and spinal motoneurons has not been demonstrated. A functional in vitro system demonstrating this connection would enable the understanding of feedback by the integration of sensory input into the spinal reflex arc. Here we report a co-culture of rat embryonic motoneurons and proprioceptive sensory neurons from dorsal root ganglia (DRG) in a defined serum-free medium on a synthetic silane substrate (DETA). Furthermore, we have demonstrated functional synapse formation in the co-culture by immunocytochemistry and electrophysiological analysis. This work will be valuable for enabling in vitro model systems for the study of spinal motor control and related pathologies such as spinal cord injury, muscular dystrophy and spasticity by improving our understanding of the integration of the mechanosensitive feedback mechanism.

Keywords

Proprioceptive sensory neurons; Dorsal root ganglion; Stretch reflex arc; Motoneurons; DETA; Serum free

1. Introduction

In vitro functional biological models are playing increasingly significant roles in both fundamental biological research and regenerative medicine. In vitro models have been reported for a plethora of systems including liver [1,2], kidney [3], skin [4,5], cardiac [6,7], lung [8], neuromuscular junction [9,10], muscle [11,12], nervous system [13,14] and

*Corresponding author. NanoScience Technology Center, 12424 Research Parkway, Suite 400, University of Central Florida, Orlando, FL 32826, USA. Tel.: +1407 823 1925; fax: +1 407 882 2819. jhickman@mail.ucf.edu (J.J. Hickman).
[1]These authors contribute equally to this work.

combinations of systems [15,16]. The reflex circuit represents the basic structure by which the central nervous system senses and responds to peripheral stimuli. The monosynaptic spinal stretch reflex circuit, a representative of the simplest reflex circuits, provides the physiological basis for fast reflexes such as the patella reflex (or knee jerk). It has been the primary model to study neural circuits, their development [17], the establishment of wiring specificity in a reflex circuit [18], as well as their mechanism of function and regulation [19–22]. The reflex circuit has also been a focus of understanding spinal cord injuries [23–25] diseases [26,27] and their treatments [28–31]. This monosynaptic circuit consists of intrafusal muscle fibers, or muscle spindles, dorsal root ganglia (DRG) Type Ia proprioceptive neurons, motoneurons and extrafusal muscle fibers. Type Ia neurons innervate the intrafusal muscle fibers via annulospiral wrappings and sense changes in the length of a muscle via activation of mechanically sensitive receptors. Activation of these receptors results in action potential generation in the Type Ia neurons which synapse onto motoneurons of the ventral spinal cord transmitting information via a glutamatergic connection [32]. The motoneuron projects to the corresponding extrafusal muscle fiber resulting in changes in muscle tension.

Although the synaptic input from Type Ia sensory neurons to motoneurons is an indispensable connection in the reflex arc, very little has been reported about the in vitro formation of this connection. Actually, very few studies report successful in vitro synapse formation between DRG neurons and spinal cord neurons [33–35]. The only studies that have accomplished in vitro formation of the specific connection between proprioceptive sensory neurons and motoneurons were reported by Streit and his colleagues but with an organotypic co-culture [35,36]. These experiments utilized a co-culture system consisting of embryonic rat spinal cord slices, DRG, and skeletal muscle, and with serum-containing media. Therefore, to our knowledge, no in vitro cell culture system has been reported that supports the co-culture of proprioceptive DRG neurons and motoneurons, with resultant synapse formation. In addition, due to the limited literature, little is known about the factors or requirements necessary for its formation in vitro.

A major goal of our laboratory has been to re-create the spinal stretch reflex arc *in vitro*. In order to accomplish this, the individual components of the circuit: intrafusal myofiber [37], DRG neurons [38], motoneurons [39] and extrafusal fibers [40,41], have been cultured in a serum-free system on a synthetic self-assembled monolayer substrate, *N*-1[3-(trimethoxysilyl)propyl] diethylenetriamine (DETA). In addition, defined co-culture systems that can support functional connections formed between several of these components: intrafusal myofibers –Type Ia sensory neurons [42] and motoneurons-myotubes [43,44] have been developed. The successful co-culture of Type Ia sensory neurons from dorsal root ganglia with embryonic motoneurons, including synaptic formation, would be the only connection missing in demonstrating the segments needed for an *in vitro* model of the stretch reflex arc. Successful completion of this elemental circuit would enable a spectrum of applications ranging from fundamental neurobiological research such as the regulation of motoneurons and spinal pattern-generating networks, the study of spinal injury/disease etiology and regenerative mechanisms, to therapeutic investigations and drug/toxin screening. These studies will also assist in fine motor control for prosthetic devices by improving our understanding of the mechano-sensory feedback mechanism.

2. Materials and methods

2.1. DETA surface preparation and characterization

Glass coverslips (VWR cat. nr. 48366067, 22 × 22 mm^2 No. 1) were chemically cleaned by using serial acid baths. First, the surfaces were soaked in a 50:50 solution of concentrated hydrochloric acid (VWR cat. nr. EM1.00314.2503) in methanol (VWR cat. nr. BJLP230-4)

for 2 h. Second, the surfaces were immersed in concentrated H_2SO_4 for at least 2 h. After each acid soak, the surfaces were carefully washed 3 times with DI water. The final water rinse was followed by boiling the glass slides in DI water for 30 min. The cleaned glass slides were placed in an oven set at 110 °C and allowed to dry overnight. The DETA (*N*-1 [3-(trimethoxysilyl) propyl]-diethylenetriamine, United Chemical Technologies Inc., Bristol, PA, T2910) monolayer was formed by the reaction of the cleaned and dried coverslips with a 0.1% (v/v) solution of the organosilane in freshly distilled toluene (VWR cat. nr. BDH1151).

Surfaces were characterized by contact angle goniometry using a Ramé Hart (Netcong, NJ) contact angle goniometer and by X-ray Photoelectron Spectroscopy (XPS) using a VG ESCALAB 220i-XL spectrometer.

2.2. Isolation of motoneurons from rat embryonic spinal cords

Rat embryonic spinal neurons were isolated from the spinal cord of day 15 embryos and embyonic motoneurons (eMNs) were then purified by density gradient followed by immunopanning with a P75 antibody [39]. This preparation protocol produces a relatively pure MN culture. In detail, the spinal cords were dissected in cold Hibernate E buffer and collected into a sterile 15 ml centrifuge tube. After one rinse with Hib E buffer, the spinal cords were digested with 0.25% trypsin (Invitrogen, Cat# 25200-056) in a 37 °C water bath for 15 min. The trypsin reaction was then quenched by adding a double volume of Hibernate E containing 20% FBS (16000-036). The tissue was then mechanically triturated with the cell suspension being transferred to a 15 ml centrifuge tube. The same process was repeated two times by adding 2 ml of Hibernate E with 20% FBS. The suspension were then pooled and centrifuged at 380*g* for 5 min. After removing the supernatant, the pellets were then resuspended into 300 μl of Hibernate E.

The Percoll density column was prepared in a 15 ml sterile conical tube as described in [43]. The panning procedure was as described in Ref. [45]. To prepare the density gradient, Optiprep (Sigma, cat# D1556-250 ml) was diluted 0.505:0.495(v/v) with Hibernate E/ GlutaMAX™/antibiotic–antimycotic/B27, and then made to 15%, 20%, 25% and 35% (v/v) from top to bottom, with 1 ml for each layer. For the panning dish, a 100 mm cell culture dish (CELLSTAR, cat# 664 160) was coated with 10 ml Goat-anti-mouse IgG (MP Biomedicals, Cat# 55479) in a 1:50 dilution with $NaHCO_3$ buffer (pH 9.5) at 4 °C overnight. After a brief rinse with PBS (pH 7.2), the coated dish was then incubated with Mouse anti-P75 antibody (Millipore, Cat# MAB365, diluted in 1:100 with PBS) at 4 °C overnight. To purify the motoneurons, the 300 μl spinal suspension was loaded on top of the density column and subjected to centrifugation at 200*g* for 15 min with zero acceleration for both the initiation and stopping phase. The top two layers of cells were collected and transferred to an immunopanning dish containing 3 ml of Hibernate E/GlutaMAX™/ antibiotic–antimycotic/B27 and incubated for 30 min at RT in a sterile environment. Then the supernatant was removed followed by 2 brief rinses of the dish with Hibernate E. The bound cells were then tapped off and collected into a 50 ml conical tube. Two more rinses with Hibernate E were conducted in order to collect all the cells from the dish. The cell suspensions were then pooled and subjected to centrifugation at 380*g* for 5 min. The cell pellet was resuspended in 1 ml of co-culture media (Table 1) and the total number of cells was counted.

2.3. Isolation of DRG neurons from rat embryonic DRGs

DRG neurons were also isolated from rat E15 embryos [38]. Proprioceptory sensory neurons were then enriched by immunopanning with the P75 antibody due to the fact that proprioceptory sensory neurons express TrkC and are NT-3 dependent [46–48], and NT-3

dependent sensory neurons express higher level of P75 than other sensory neurons [49]. In detail, DRGs were dissected in cold Hibernate E buffer and were digested with 0.25% trypsin (Invitrogen, Cat# 25200-056) in a 37 °C water bath for 12 min. The trypsin reaction was quenched by adding a double volume of Hibernate E containing 20% FBS (16000-036). The tissue was then mechanically triturated with the cell suspension being transferred to a 15 ml centrifuge tube. The suspension was centrifuged at 380*g* for 5 min. After removing the supernatant, the pellets were resuspended into 300 μl of Hibernate E. The immunopanning dish with the P75 antibody was prepared as described above. The cell suspension from the DRG prep was transferred to a panning dish containing 5 ml of Hibernate E followed by 25 min of incubation at RT. Then the dish was rinsed and the bound cells were collected and counted as above.

2.4. Co-culture of DRG cells and motoneurons

Purified DRG neurons and motoneurons were plated simultaneously at a density of 200 cells/mm^2 and 75 cells/mm^2, respectively, on the DETA surfaces in a novel defined serum-free culture medium (Table 1). To eliminate contaminating Schwann cells from the DRG preparation, co-cultures were treated with antimitotics (10^{-5} M fluorodeoxyuridine (FdU, Sigma, Cat# F0503) and 10^{-5} M uridine (Sigma, Cat# U3003)) for 3 days beginning on day 2 of culture. Then the co-cultures were fed with co-culture media on day 4 and every 3 days thereafter by changing half of the media. Co-cultures were monitored with phase microscopy. After approximately 7 days, co-cultures were analyzed by both immunocytochemistry and electrophysiology.

2.5. Immunocytochemistry

Immunostaining was conducted as described in Ref. [50]. Briefly, cells on DETA coverslips were fixed in freshly prepared 4% paraformaldehyde for 15 min. Cells were then washed twice in Phosphate Buffered Saline (PBS, pH 7.2) for 10 min each at room temperature, and permeabilized with 0.1% Triton X-100/PBS for 15 min. Non-specific binding sites were blocked with 5% Donkey serum plus 0.5% BSA in PBS (Blocking buffer) for 45 min at room temperature. Cells were then incubated with primary antibodies overnight at 4 °C. After being washed with PBS 3× for 10 min, the cells were incubated with secondary antibodies for 2.5 h at room temperature. The cells were then washed with PBS 3× for 10 min and mounted with Vectashield with 4′-6-diamidino-2-phenylindole (dapi) (Vector laboratories, Inc.). The primary antibodies utilized in this study were: Guinea pig-anti-parvalbumin (Chemicon, 1:300) for Type Ia sensory neurons, Rabbit-anti-MAP2 (Chemicon, 1:1000) for all the neurons, and mouse anti-synaptophysin (Antibodies Inc., 1:100) for pre-synaptic terminals. Secondary antibodies included: Donkey-anti-Gp-568 (Invitrogen, 1:250), Donkey-anti-Mouse-488 (Invitrogen, 1:250), Donkey-anti-Rabbit-594 (Invitrogen, 1:250). All antibodies were diluted in blocking buffer.

2.6. Electrophysiology

DRG and motoneurons were co-cultured on DETA coated coverslips 7–10 days prior to electrophysiological characterization. Type Ia sensory neurons or motoneurons were selected for patch-clamp analysis based on morphology under an infrared DIC-video microscope. The largest multipolar or round cells (15–30 μm diam) with bright illuminance in the culture were tentatively identified as motoneurons [50–52]. Compared to motoneurons, sensory neurons were generally very distinctive because their soma tended to bulge above the surface and their processes tended to fasciculate. In addition, Type Ia sensory neurons were usually larger than other types of sensory neurons [53] and were selected on this basis. Whole-cell, patch-clamp recordings were performed in a recording chamber that was placed on the stage of a Zeiss Axioscope, 2 FS Plus, upright microscope. The chamber was filled with room temperature extracellular solution composed of (in mM):

120 NaCl, 1.2 KH_2PO_4, 1.9 KCl, 26 $NaHCO_3$, 10 D-glucose, 7.5 HEPES, 2.2 $CaCl_2$, and $MgSO_4$. Patch pipettes (6–8 MΩ) were pulled from thick-walled borosilicate glass (BF 150-86-10; Sutter, Novato, CA) with a Flaming Brown P97 Pipette Puller (Sutter Instrument Company). Patch pipettes were filled with intracellular solution (in mM): 140 K-gluconate, 1 ethylene glycol-bis[aminoethylether]-tetra-acetic acid, 2 $MgCl_2$, 5 Na_2ATP, 10 HEPES; pH 7.2. After the formation of a gigaohm seal between the patch pipettes and the cell membrane, the membrane was punctured and the cell capacitance was compensated. The series resistance was typically <23 MΩ, and it was compensated >60% using the amplifier circuitry. Signals were filtered at 3 kHz and sampled at 20 kHz using a Digidata 1322A interface (Axon instrument). Voltage and current-clamp experiments were performed with a Multiclamp 700A (Axon, Union City, CA) amplifier. Data recordings and analysis were performed with pClamp8 (Axon) software. Membrane resistance and capacitance were calculated using 50 ms voltage steps from −85 to −95 mV without any whole-cell or series resistance compensation. The resting membrane potential and depolarization-evoked action potentials were recorded in current-clamp mode. Depolarization-evoked inward and outward currents were examined in voltage-clamp mode. Miniature excitatory postsynaptic currents (mEPSCs) were recorded in gap-free mode from motoneurons in voltage-clamp mode at a holding potential of −70 mV.

2.7. Blocking of mEPSCs with CNQX and D-AP5

To test whether the recorded MN receive any glutamatergic synaptic input, GAP-free mode was allowed to run for ~2 min. If any mEPSCs were recorded, the concentrated glutamate receptor antagonists CNQX (final 20 μM, 6-Cyano-7-nitroquinoxaline-2,3-dione disodium, Tocris, Cat. No 1045) and D-AP5 (final 20 μM, D-(−)-2-amino-5-phosphonovaleric acid, Tocris, Cat. No 0106) were added to the recording chamber acutely, and the cells were recorded for another 3 min in Gap-free mode.

3. Results

3.1. DETA surface characterization

The self-assembled monolayer formed by the aminosilane, trimethoxy-silylpropyl-diethylenetriamine (DETA), can function efficiently as a non-biological substrate, and is an ideal surface for neuronal cellular attachment and survival [54–57]. XPS measurements of the DETA coated coverslips indicated a complete monolayer formed after the self-assembly process (Fig. 1A). The normalized area values of N1s (401 and 399 eV) to the Si $2p_{3/2}$ peaks were stable throughout the study at 1300–2300 and were similar to previously published results [38,39,43,58,59]. Static contact angle measurements (Fig. 1B) of 45.6 ± 2° validated the hydrophilicity of the DETA surfaces. Stable XPS readings and contact angles across coverslips throughout the study indicate uniformity and reproducibility of the self-assembly of the DETA monolayer.

3.2. Phase microscopic observation of the co-culture DRG sensory neurons and motoneurons

Observation through phase contrast microscopy indicated morphologically healthy and well distinguished motoneurons (red arrows) and DRG sensory neurons (green arrows) (Fig. 2). Motoneurons were usually polygonal, had thick and long axons, multiple dendrites, and large soma with a diameter of 15–30 μm [50–52]. DRG neurons were generally round, large, bi-polar (having two processes), and their processes tended to fasciculate. Under the microscope, their somas typically bulged above the surface and appeared phase bright.

3.3. Immunocytochemical analysis of Type Ia sensory neurons and motoneurons in the co-culture

Immunocytochemistry was utilized to analyze the Type Ia sensory neurons and motoneurons in the co-culture. Type Ia sensory neurons were stained with the marker Parvalbumin, a calcium-binding protein which stains the Type Ia proprioceptive population in DRG neurons [38,47,53,60]. Most of the DRG neurons in the culture were Parvalbumin-positive. Since Parvalbumin only stains the soma, the general neuronal marker MAP2 was used to reveal all the detail of the processes for both motoneurons and sensory neurons. Motoneurons were identified by their typical morphology [50–52]. Co-immunostaining of Parvalbumin and MAP2 demonstrated the presence of motoneurons and Type Ia sensory neurons in the co-culture and the physical contacts between them through their processes (Fig. 3).

3.4. Electrophysiological analysis of large sensory neurons and motoneurons in the co-culture

Since proprioceptive neurons generally have a large soma size and thick axons [53], and are very bright under a phase microscope, this population of sensory neurons were visually identified and analyzed. Similarly, motoneurons were visually identified based on their large, polygonal soma and thick axons [50–52]. Only those cells with a soma diameter above 20 μm were chosen for analysis to make certain only motoneurons were selected. Both sensory neurons and embryonic motoneurons exhibited inward and outward currents and repetitive firing in the co-culture that were characteristic of functionally mature neurons. (Fig. 4, Table 2).

3.5. Immunocytochemical characterization of the DRG–motoneuron synapse

In order to determine if synapses between the MN and Type Ia sensory neurons occurred in the defined culture system, the cells were immunostained with synaptophysin (a synaptic vesicle protein) as a pre-synaptic marker of synapse formation. Co-immunostaining with synaptophysin and MAP2 revealed that abundant synaptic terminals of the parvalbumin-positive sensory neurons wrapped around the MNs in both the soma and dendritic regions. Co-immunostaining also indicated that synaptophysin signals were concentrated at the contact spots between MN dendrites and passing processes which were potentially from sensory neurons (Fig. 5), strongly suggesting synaptic formation at these sites. Although motoneurons also receive monosynaptic inputs from descending systems such as the vestibulospinal tract and multiple types of descending sensory and locomotor inputs, mediated by a wide range of interneurons, and even from motoneurons in some in vitro conditions, they were unlikely to occur in our culture system, as explained in Section 4. Thus all the evidence for synaptic connections could safely be ascribed to synapses between Type Ia sensory neurons and motoneurons.

3.6. Electrophysiological characterization of the DRG–motoneuron synapse

To determine if the synapses between these two neuronal cell types identified by immunocytochemistry were functional, miniature EPSCs (mEPSCs) from motoneurons in co-culture were recorded. mEPSCs occur in the postsynaptic cell (motoneuron) in response to quantal release of neurotransmitter from the pre-synaptic neurons and are therefore indicative of synapse formation. In vivo, Type Ia input is the only direct monosynaptic connection from sensory afferents to motoneurons [20,32]. mEPSCs were recorded in voltage-clamp mode at a holding potential of −70 mV. Average mEPSC amplitude was −55.5 ± 16.9 pA and average frequency was 0.4 ± 0.08 Hz. Acute application of CNQX (20 μM) and D-AP5 (20 μM) almost completely blocked the occurrence of mEPSCs. The blocking of mEPSCs by the acute application of the antagonists of Glutamate receptors

indicated that these synapses were both functional and glutamatergic as expected for a Type Ia sensory to motoneuron synapse (Fig. 6).

4. Discussion

This study reports a novel defined in vitro cell culture system that supports the growth and differentiation of a functional co-culture of proprioceptive DRG neurons and spinal motoneurons. Functional synapse formation between proprioceptive sensory neurons and motoneurons was demonstrated utilizing both immunocytochemistry and electrophysiological analysis. This in vitro co-culture model can now facilitate the study of the parameters for connectivity between DRG neurons and motoneurons and its later incorporation into the complete reflex arc circuit.

The in vivo neural networks associated with DRG neurons and spinal motoneurons are very complicated, and our system provides a simplified model to study this monosynaptic connection. It is called monosynaptic because the synaptic connection between the sensory neurons and the motoneurons is direct, without the mediation of any interneurons. Normally, DRG neurons collect sensory information from various sensory receptors in the periphery and relay them to the central nervous system (CNS) via their central axons. Specifically, DRG neurons that transmit nociception and thermoception project to the superficial layers of the dorsal horn, whereas those transmitting mechanoreception project to the deeper layers. Three types of proprioceptive DRG neurons provide information about muscle length and tension to the spinal cord. Group Ia and II afferent axons innervate muscle spindles, and group Ib afferent axons innervate Golgi tendon organs in the periphery. Group Ia afferents form monosynapses on homonymous motoneurons and complete the simplest stretch reflex circuits. Group Ib and II afferents form oligo-/or poly-synaptic connections onto spinal motoneurons [20,32]. Although there are some studies reporting the monosynaptic formation onto motoneurons from type II afferents [61], its contribution to the stretch reflex is very small [20,62] and usually is ignored when considering proprioceptive input onto α-motoneurons [63], the neurons that normally receive monosynaptic inputs from DRG. In our culture, Type Ia sensory neurons were enriched compared to other sensory neurons with the P75 immunopanning procedure. Thus, Type Ia sensory neurons were the dominant group of neurons from DRGs that form monosynapses on motoneurons in vivo and even more so in our culture.

On the other hand, spinal motoneurons receive two major groups of synaptic inputs in vivo. One group is the descending tracts from supra-spinal motor centers [64–67], which were not present in our culture system. The other group is from the spinal circuits established by the proprioceptive afferents from muscle spindle and Golgi tendon in the muscles, as well as the spinal recurrent inhibition via Renshaw cells [20]. In our culture, motoneurons were purified from the whole spinal cord prep by a gradient column and immunopanning. More than 90% of the cells were motoneurons after these procedures based on Islet1 immunocytochemistry [39]. Similarly, our observations under phase contrast microscopy did not find any interneuron-like cells and all the neurons in the co-culture exhibited morphology consistent with either motoneurons or DRG neurons. Thus, the number of interneurons in our culture system would be either extremely low or non-existent. Therefore, the mEPSCs recorded from motoneurons were unlikely from interneuron input. Correspondingly, no inhibitory postsynaptic currents (mIPSCs) were observed during the recordings of PSCs. This also implied the absence of interneurons in the co-culture, since IPSCs can only be from interneuron inputs. As a result, the lack of interneurons in our co-culture would eliminate the oligo- or poly-synaptic connections between DRG neurons and motoneurons, leaving only monosynaptic connections possible. Although synapse formation between spinal motoneurons has been reported, it would be a rare occurrence in the absence of glia cells

[68]. The application of antimitotics removed almost all the glia cells in our system and made interneuron-motoneuron connections improbable. In general, with the purified motoneurons, enriched Type Ia sensory neurons and the removal of glial cells, we have established a model system that favors the monosynaptic connection between Type Ia sensory neurons and α-motoneurons. This system is ideal for the study of the simplest stretch reflex mechanism and its regulation.

This study utilized a defined, serum-free medium which supports the growth and differentiation of proprioceptive sensory neurons and motoneurons as well as synapse formation. The medium consists of the M1 media plus NGF. NGF is an essential factor for the survival and differentiation of sensory neurons [49,69]. Our previous study associated with the reflex arc indicated that M1 media supports the co-culture of spinal motoneurons and skeletal myotubes and corresponding neuromuscular junction (NMJ) formation [43]. The addition of 12 new growth factors (M2) known to increase NMJ formation and synaptic maintenance has greatly enhanced rat NMJ formation in a defined system [44]. Similarly, the addition of NGF to the combination of M1 and M2 was shown to support the sensory neuron innervations of intrafusal muscle fibers [42]. This study indicates that the addition of NGF to M1 alone can support the synapse formation between proprioceptive sensory neurons and motoneurons. This result strongly suggests that this media system is compatible to other media systems for the building of the reflex arc. In addition, the defined composition enables this system to be feasible for dissecting the individual factors and the investigation of the underlying mechanisms when studying the monosynaptic spinal reflex. In general, the elucidation of these media systems would facilitate the development of functional in vitro systems for the study of motor control and related pathologies such as spinal cord injuries and spasticity as well as their treatment. These studies will also assist in engineering fine motor control for prosthetic devices by improving our understanding of the monosynaptic reflex arc.

The engineered synthetic substrate DETA has previously been shown to support neuronal [39], skeletal muscle [41], endothelial [70], and cardiac cell growth [71], and had been used in creating high resolution, in vitro patterned circuits of embryonic hippocampal neurons [55]. The patterning of DETA surface with SAM technologies has been shown to promote guided axonal growth and direct axonal and dendritic process extension at the level of a single neuron [57]. This synthesized surface is also compatible with Bio-MEMs devices such as MEAs [72] and cantilevers [12], implying their future integration into the next generation of high throughput screening technologies. Therefore, the successful culture on this substrate suggests that this co-culture can be patterned at high resolution to build engineered neural networks. Considering previous studies indicated that DETA supported the growth and differentiation of spinal motoneurons [39], skeletal muscles [40], DRG neurons [38], as well as the synaptic connections between MN-skeletal muscle and skeletal muscle-DRG neurons [44], the successful culture of DRG neurons and motoneurons and their synapse formation highlights the possibility of establishing the complete spinal reflex arc on patterned DETA surfaces. This would allow a high-resolution reflex arc neural network to be built and its development into a high content and ultimately high throughput screening system for drug discovery.

5. Conclusion

In summary, this study reports the co-culture of proprioceptive sensory neurons and spinal motoneurons as well as functional synapse formation. The simplified network in the co-culture would facilitate the study of the regulation and interaction of Type Ia sensory neurons and motoneurons, thus the prioproceptive sensory pathway and the development of the complete reflex arc in vitro. The defined nature of this system and its compatibility with

the DETA non-biological substrate, make it amenable to multiple applications ranging from fundamental neurobiological research, to the development of in vitro neural networks for high throughput drug screening, as well as the design of prosthetic devices.

Acknowledgments

"The project described was supported by Grant Numbers R01NS050452 from the National Institute of Neurological Disorders And Stroke and R01EB009429 from the National Institute of Biomedical Imaging and Bioengineering. The content is solely the responsibility of the authors and does not necessarily represent the official views of the National Institute of Neurological Disorders and Stroke, the National Institute of Biomedical Imaging and Bioengineering or the National Institutes of Health." We thank Christopher McAleer for constructively reviewing the manuscript. The authors confirm that no competing financial interests exist and there has been no financial support for this research that could have influenced its outcome.

References

1. Groneberg DA, Grosse-Siestrup C, Fischer A. In vitro models to study hepatotoxicity. Toxicol Pathol. 2002; 30:394–9. [PubMed: 12051557]
2. Cai J, Zhao Y, Liu Y, Ye F, Song Z, Qin H, et al. Directed differentiation of human embryonic stem cells into functional hepatic cells. Hepatology. 2007; 45:1229–39. [PubMed: 17464996]
3. Subramanian B, Rudym D, Cannizzaro C, Perrone R, Zhou J, Kaplan DL. Tissue-engineered three-dimensional in vitro models for normal and diseased kidney. Tissue Eng Part A. 2010; 16:2821–31. [PubMed: 20486787]
4. Schlüter H, Kaur P. Bioengineered human skin from embryonic stem cells. The Lancet. 2009; 374:1725–6.
5. Guenou H, Nissan X, Larcher F, Feteira J, Lemaitre G, Saidani M, et al. Human embryonic stem-cell derivatives for full reconstruction of the pluristratified epidermis: a preclinical study. The Lancet. 2009; 374:1745–53.
6. Smits AM, van Vliet P, Metz CH, Korfage T, Sluijter JPG, Doevendans PA, et al. Human cardiomyocyte progenitor cells differentiate into functional mature cardiomyocytes: an in vitro model for studying human cardiac physiology and pathophysiology. Nat Protoc. 2009; 4:232–43. [PubMed: 19197267]
7. Matsa E, Rajamohan D, Dick E, Young L, Mellor I, Staniforth A, et al. Drug evaluation in cardiomyocytes derived from human induced pluripotent stem cells carrying a long QT syndrome type 2 mutation. Eur Heart J. 2011; 32:952–62. [PubMed: 21367833]
8. Huh D, Matthews BD, Mammoto A, Montoya-Zavala Mn, Hsin HY, Ingber DE. Reconstituting organ-level lung functions on a chip. Science. 2010; 328:1662–8. [PubMed: 20576885]
9. Guo X, Das M, Rumsey J, Gonzalez M, Stancescu M, Hickman J. Neuromuscular junction formation between human stem-cell-derived motoneurons and rat skeletal muscle in a defined system. Tissue Eng Part C Methods. 2010; 16:1347–55. [PubMed: 20337513]
10. Guo X, Gonzalez M, Stancescu M, Vandenburgh HH, Hickman JJ. Neuromuscular junction formation between human stem cell-derived motoneurons and human skeletal muscle in a defined system. Biomaterials. 2011; 32:9602–11. [PubMed: 21944471]
11. Wilson K, Molnar P, Hickman J. Integration of functional myotubes with a Bio-MEMS device for non-invasive interrogation. Lab Chip. 2007; 7:920–2. [PubMed: 17594013]
12. Wilson K, Das M, Wahl KJ, Colton RJ, Hickman J. Measurement of contractile stress generated by cultured rat muscle on silicon cantilevers for toxin detection and muscle performance enhancement. PLoS One. 2010; 5:e11042. [PubMed: 20548775]
13. Frampton JP, Shuler ML, Shain W, Hynd MR. Biomedical technologies for in vitro screening and controlled delivery of neuroactive compounds. Cent Nerv Syst Agents Med Chem. 2008; 8:203–19. [PubMed: 19079777]
14. Frampton J, Hynd M, Shuler M, Shain W. Effects of glial cells on electrode impedance recorded from neural prosthetic devices in vitro. Ann Biomed Eng. 2010; 38:1031–47. [PubMed: 20336824]

15. Esch MB, King TL, Shuler ML. The role of body-on-a-chip devices in drug and toxicity studies. Annu Rev Biomed Eng. 2011; 13:55–72. [PubMed: 21513459]
16. Sung JH, Shuler ML. A micro cell culture analog (microCCA) with 3-D hydrogel culture of multiple cell lines to assess metabolism-dependent cytotoxicity of anti-cancer drugs. Lab Chip. 2009; 9:1385–94. [PubMed: 19417905]
17. Chen HH, Hippenmeyer S, Arber S, Frank E. Development of the monosynaptic stretch reflex circuit. Curr Opin Neurobiol. 2003; 13:96–102. [PubMed: 12593987]
18. Maro GS, Shen K, Cheng H-J. Deal breaker: semaphorin and specificity in the spinal stretch reflex circuit. Neuron. 2009; 63:8–11. [PubMed: 19607788]
19. Schomburg ED. Spinal sensorimotor systems and their supraspinal control. Neurosci Res. 1990; 7:265–340. [PubMed: 2156196]
20. Windhorst U. Muscle proprioceptive feedback and spinal networks. Brain Res Bull. 2007; 73:155–202. [PubMed: 17562384]
21. Hultborn H. Spinal reflexes, mechanisms and concepts: from eccles to lundberg and beyond. Prog Neurobiol. 2006; 78:215–32. [PubMed: 16716488]
22. Boggs JW, Wenzel BJ, Gustafson KJ, Grill WM. Spinal micturition reflex mediated by afferents in the deep perineal nerve. J Neurophysiol. 2005; 93:2688–97. [PubMed: 15601736]
23. Nakazawa K, Kawashima N, Akai M. Enhanced stretch reflex excitability of the soleus muscle in persons with incomplete rather than complete chronic spinal cord injury. Arch Phys Med Rehabil. 2006; 87:71–5. [PubMed: 16401441]
24. Dietz V, Grillner S, Trepp A, Hubli M, Bolliger M. Changes in spinal reflex and locomotor activity after a complete spinal cord injury: a common mechanism? Brain. 2009; 132:2196–205. [PubMed: 19460795]
25. Norton JA, Bennett DJ, Knash ME, Murray KC, Gorassini MA. Changes in sensory-evoked synaptic activation of motoneurons after spinal cord injury in man. Brain. 2008; 131:1478–91. [PubMed: 18344559]
26. Britton, T.; Maria, SPhDM. Abnormalities of muscle tone and movement. In: Stokes, M., editor. Physical management in neurological rehabilitation. 2. Oxford: Mosby; 2004. p. 47-56.
27. Jiang M, Schuster JE, Fu R, Siddique T, Heckman CJ. Progressive changes in synaptic inputs to motoneurons in adult sacral spinal cord of a mouse model of amyotrophic lateral sclerosis. J Neurosci. 2009; 29:15031–8. [PubMed: 19955354]
28. Barbeau H, McCrea DA, O'Donovan MJ, Rossignol S, Grill WM, Lemay MA. Tapping into spinal circuits to restore motor function. Brain Res Brain Res Rev. 1999; 30:27–51. [PubMed: 10407124]
29. Garrison MK, Yates CC, Reese NB, Skinner RD, Garcia-Rill E. Wind-up of stretch reflexes as a measure of spasticity in chronic spinalized rats: the effects of passive exercise and modafinil. Exp Neurol. 2010; 227:104–9. [PubMed: 20932828]
30. Fairchild MD, Kim SJ, Iarkov A, Abbas JJ, Jung R. Repetetive hindlimb movement using intermittent adaptive neuromuscular electrical stimulation in an incomplete spinal cord injury rodent model. Exp Neurol. 2010; 223:623–33. [PubMed: 20206164]
31. Courtine G, Gerasimenko Y, van den Brand R, Yew A, Musienko P, Zhong H, et al. Transformation of nonfunctional spinal circuits into functional states after the loss of brain input. Nat Neurosci. 2009; 12:1333–42. [PubMed: 19767747]
32. Rekling JC, Funk GD, Bayliss DA, Dong X-W, Feldman JL. Synaptic control of motoneuronal excitability. Physiol Rev. 2000; 80:767–852. [PubMed: 10747207]
33. Joseph DJ, Choudhury P, Macdermott AB. An in vitro assay system for studying synapse formation between nociceptive dorsal root ganglion and dorsal horn neurons. J Neurosci Methods. 2010; 189:197–204. [PubMed: 20385165]
34. Ohshiro H, Ogawa S, Shinjo K. Visualizing sensory transmission between dorsal root ganglion and dorsal horn neurons in co-culture with calcium imaging. J Neurosci Methods. 2007; 165:49–54. [PubMed: 17597226]
35. Spenger C, Braschler UF, Streit J, Lüscher H-R. An organotypic spinal cord-dorsal root ganglion-skeletal muscle coculture of embryonic rat. I. The morphological correlates of the spinal reflex arc. Eur J Neurosci. 1991; 3:1037–53. [PubMed: 12106236]

36. Streit J, Spenger C, Lüscher H-R. An organotypic spinal cord-dorsal root ganglion-skeletal muscle coculture of embryonic rat. II. Functional evidence for the formation of spinal reflex arcs in vitro. Eur J Neurosci. 1991; 3:1054–68. [PubMed: 12106237]
37. Rumsey JW, Das M, Kang J-F, Wagner R, Molnar P, Hickman JJ. Tissue engineering intrafusal fibers: dose- and time-dependent differentiation of nuclear bag fibers in a defined in vitro system using neuregulin 1-[beta]-1. Biomaterials. 2008; 29:994–1004. [PubMed: 18076984]
38. Liu J, Rumsey JW, Das M, Molnar P, Gregory C, Riedel L, et al. Electrophysiological and immunocytochemical characterization of DRG neurons on an organosilane surface in serum-free medium. Vitro Cell Dev Biol Animal. 2008; 44:162–8.
39. Das M, Molnar P, Devaraj H, Poeta M, Hickman JJ. Electrophysiological and morphological characterization of rat embryonic motoneurons in a defined system. Biotechnol Prog. 2003; 19:1756–61. [PubMed: 14656152]
40. Das M, Rumsey JW, Bhargava N, Stancescu M, Hickman JJ. Skeletal muscle tissue engineering: a maturation model promoting long-term survival of myotubes, structural development of the excitation-contraction coupling apparatus and neonatal myosin heavy chain expression. Biomaterials. 2009; 30:5392–402. [PubMed: 19625080]
41. Das M, Gregory CA, Molnar P, Riedel LM, Wilson K, Hickman JJ. A defined system to allow skeletal muscle differentiation and subsequent integration with silicon microstructures. Biomaterials. 2006; 27:4374–80. [PubMed: 16647113]
42. Rumsey JW, Das M, Bhalkikar A, Stancescu M, Hickman JJ. Tissue engineering the mechanosensory circuit of the stretch reflex arc: sensory neuron innervation of intrafusal muscle fibers. Biomaterials. 2010; 31:8218–27. [PubMed: 20708792]
43. Das M, Rumsey JW, Gregory CA, Bhargava N, Kang JF, Molnar P, et al. Embryonic motoneuron-skeletal muscle co-culture in a defined system. Neuroscience. 2007; 146:481–8. [PubMed: 17383103]
44. Das M, Rumsey JW, Bhargava N, Stancescu M, Hickman JJ. A defined long-term in vitro tissue engineered model of neuromuscular junctions. Biomaterials. 2010; 31:4880–8. [PubMed: 20346499]
45. Camu W, Henderson CE. Purification of embryonic rat motoneurons by panning on a monoclonal antibody to the low-affinity NGF receptor. J Neurosci Methods. 1992; 44:59–70. [PubMed: 1434751]
46. Barbacid M. The Trk family of neurotrophin receptors. J Neurobiol. 1994; 25:1386–403. [PubMed: 7852993]
47. Ernfors P, Lee K-F, Kucera J, Jaenisch R. Lack of neurotrophin-3 leads to deficiencies in the peripheral nervous system and loss of limb proprioceptive afferents. Cell. 1994; 77:503–12. [PubMed: 7514502]
48. Klein R, Silos-Santiago I, Smeyne RJ, Lira SA, Brambilla R, Bryant S, et al. Disruption of the neurotrophin-3 receptor gene trkC eliminates la muscle afferents and results in abnormal movements. Nature. 1994; 368:249–51. [PubMed: 8145824]
49. Barrett GL, Georgiou A, Reid K, Bartlett PF, Leung D. Rescue of dorsal root sensory neurons by nerve growth factor and neurotrophin-3, but not brain-derived neurotrophic factor or neurotrophin-4, is dependent on the level of the p75 neurotrophin receptor. Neuroscience. 1998; 85:1321–8. [PubMed: 9681965]
50. Guo X, Johe K, Molnar P, Davis H, Hickman J. Characterization of a human fetal spinal cord stem cell line, NSI-566RSC, and its induction to functional motoneurons. J Tissue Eng Regen Med. 2010; 4:181–93. [PubMed: 19950213]
51. Gao BX, Ziskind-Conhaim L. Development of glycine- and GABA-gated currents in rat spinal motoneurons. J Neurophysiol. 1995; 74:113–21. [PubMed: 7472315]
52. Takahashi T. Intracellular recording from visually identified motoneurons in rat spinal cord slices. Proc Roy Soc Lond B Biol Sci. 1978; 202:417–21. [PubMed: 29296]
53. Carr PA, Yamamoto T, Karmy G, Baimbridge KG, Nagy JI. Parvalbumin is highly colocalized with calbindin D28k and rarely with calcitonin gene-related peptide in dorsal root ganglia neurons of rat. Brain Res. 1989; 497:163–70. [PubMed: 2790451]

54. Schaffner AE, Barker JL, Stenger DA, Hickman JJ. Investigation of the factors necessary for growth of hippocampal neurons in a defined system. J Neurosci Methods. 1995; 62:111–9. [PubMed: 8750092]
55. Ravenscroft MS, Bateman KE, Shaffer KM, Schessler HM, Jung DR, Schneider TW, et al. Developmental neurobiology implications from fabrication and analysis of hippocampal neuronal networks on patterned silane-modified surfaces. J Am Chem Soc. 1998; 120:12169–77.
56. Stenger DA, Pike CJ, Hickman JJ, Cotman CW. Surface determinants of neuronal survival and growth on self-assembled monolayers in culture. Brain Res. 1993; 630:136–47. [PubMed: 8118680]
57. Stenger DA, Hickman JJ, Bateman KE, Ravenscroft MS, Ma W, Pancrazio JJ, et al. Microlithographic determination of axonal/dendritic polarity in cultured hippocampal neurons. J Neurosci Methods. 1998; 82:167–73. [PubMed: 9700689]
58. Molnar P, Kang JF, Bhargava N, Das M, Hickman JJ. Synaptic connectivity in engineered neuronal networks. Methods Mol Biol. 2007; 403:165–73. [PubMed: 18827993]
59. Rumsey JW, Das M, Stancescu M, Bott M, Fernandez-Valle C, Hickman JJ. Node of Ranvier formation on motoneurons in vitro. Biomaterials. 2009; 30:3567–72. [PubMed: 19361859]
60. Nagano I, Shapshak P, Yoshioka M, Xin KQ, Nakamura S, Bradley WG. Parvalbumin and calbindin D-28 k immunoreactivity in dorsal root ganglia in acquired immunodeficiency syndrome. Neuropathol Appl Neurobiol. 1996; 22:293–301. [PubMed: 8875463]
61. Kirkwood PA, Sears TA. Monosynaptic excitation of motoneurones from secondary endings of muscle spindles. Nature. 1974; 252:243–4. [PubMed: 4278994]
62. Stauffer EK, Watt DG, Taylor A, Reinking RM, Stuart DG. Analysis of muscle receptor connections by spike-triggered averaging. 2. Spindle group II afferents. J Neurophysiol. 1976; 39:1393–402. [PubMed: 136501]
63. Kanning KC, Kaplan A, Henderson CE. Motor neuron diversity in development and disease. Annu Rev Neurosci. 2010; 33:409–40. [PubMed: 20367447]
64. Lemon, RN.; Kirkwood, PA.; Maier, MA.; Nakajima, K.; Nathan, P. Direct and indirect pathways for corticospinal control of upper limb motoneurons in the primate. In: Mori, S.; Stuart, DG.; Wiesendanger, M., editors. Progress in brain research. New York: Elsevier; 2004. p. 263-79.
65. Holstege G. The anatomy of the central control of posture: consistency and plasticity. Neurosci Biobehav Rev. 1998; 22:485–93. [PubMed: 9595559]
66. Cheney, PD.; Fetz, EE.; Mewes, K. Neural mechanisms underlying corticospinal and rubrospinal control of limb movements. In: Holstege, G., editor. Progress in brain research. New York: Elsevier; 1991. p. 213-52.[chapter 11]
67. Lemon RN. Descending pathways in motor control. Annu Rev Neurosci. 2008; 31:195–218. [PubMed: 18558853]
68. Ullian EM, Harris BT, Wu A, Chan JR, Barres BA. Schwann cells and astrocytes induce synapse formation by spinal motor neurons in culture. Mol Cell Neurosci. 2004; 25:241–51. [PubMed: 15019941]
69. Johnson EM Jr, Rich KM, Yip HK. The role of NGF in sensory neurons in vivo. Trends Neurosci. 1986; 9:33–7.
70. Spargo BJ, Testoff MA, Nielsen TB, Stenger DA, Hickman JJ, Rudolph AS. Spatially controlled adhesion, spreading, and differentiation of endothelial cells on self-assembled molecular monolayers. PNAS. 1994; 91:11070–4. [PubMed: 7972011]
71. Das M, Molnar P, Gregory C, Riedel L, Hickman JJ. Long-term culture of embyonic rat cardiomyocytes on an organosilane surface in a serum free medium. Biomaterials. 2004; 25:5643–7. [PubMed: 15159080]
72. Varghese K, Molnar P, Das M, Bhargava N, Lambert S, Kindy MS, et al. A new target for amyloid beta toxicity validated by standard and high-throughput electrophysiology. PLoS One. 2010; 5:e8643. [PubMed: 20062810]

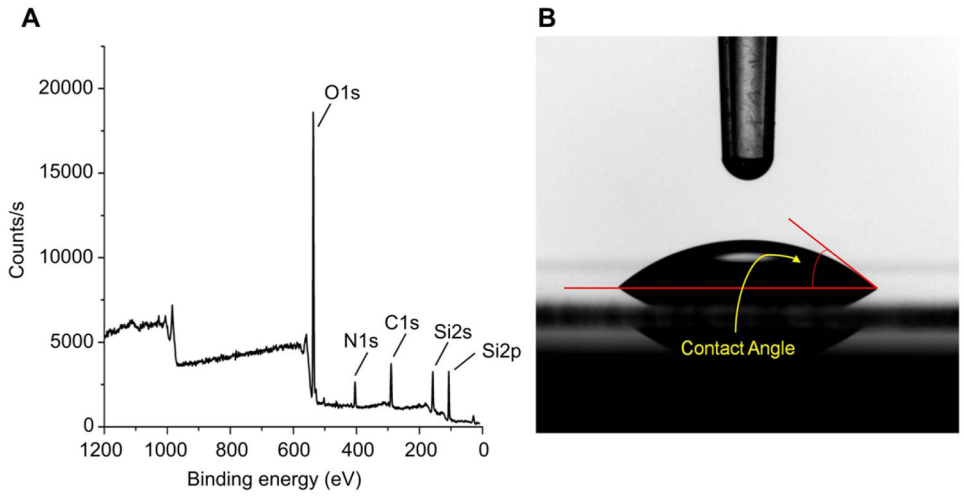

Fig. 1.

Surface characterization of a DETA monolayer on glass coverslips. (A) XPS survey spectra analysis of the DETA coverslip. (B) Contact angle measurement image of water on a DETA coverslip.

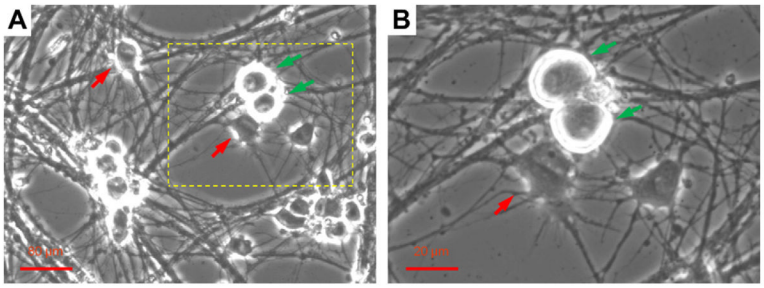

Fig. 2.
Phase contrast image of examples of motoneurons (red arrows) and Type Ia sensory neurons (green arrow) in the co-culture identified by typical morphology. Pictures were taken from a day 12 culture. B is a four-fold amplified image of A demonstrating the area outlined with dotted lines.

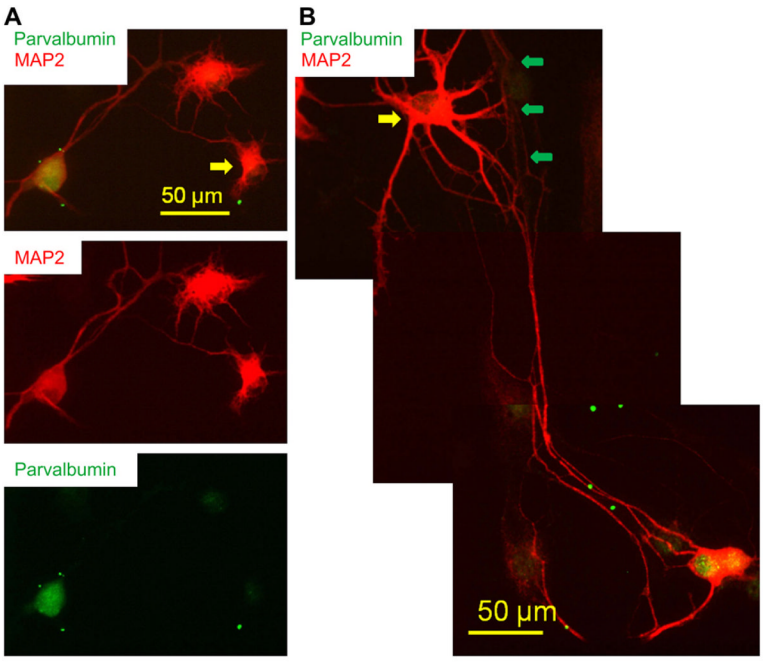

Fig. 3.

Immunocytochemistry analysis of a day 12 co-culture. (A) Co-immunostaining of Parvalbumin and MAP2. Antibodies to MAP2 (red) demonstrated all the neurons in the culture with the details of their processes. Antibody to parvalbumin (green) labels Type Ia sensory neurons. Motoneurons can be visually identified by their featured morphology (yellow arrows). The neural fibers sent out by the sensory neurons tended to fasciculate and travel long distances in the culture. (B) Abundant contacts between the dendrites of motoneurons and passing neural fiber tracts can be observed (green arrows).

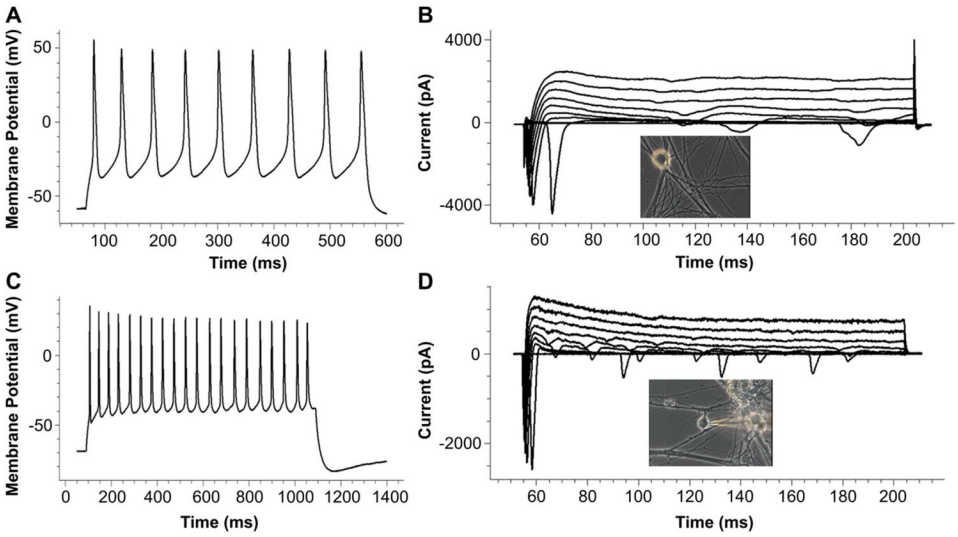

Fig. 4.

Patch-clamp recordings from DRG neurons and motoneurons in the co-culture. (A) An example trace of a repetitive action potential recorded from a Type Ia sensory neuron in a day 13 co-culture. (B) An example of active Na^+ (inward) and K^+ (outward) currents recorded from the same Type Ia sensory neuron as in A. The insert picture indicates the recorded neuron. (C and D) Example recordings of a repetitive action potential (C) and active Na^+ (inward) and K^+ (outward) currents (D) from a motoneuron in a day 11 co-culture.

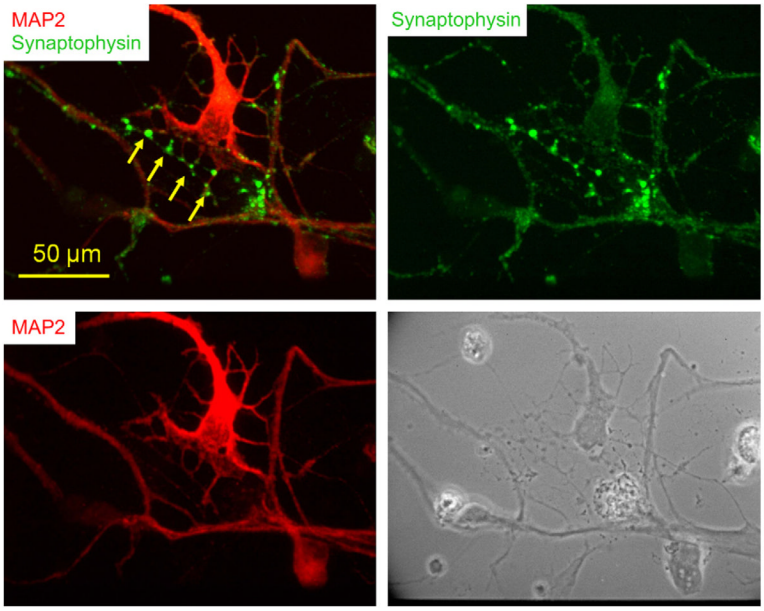

Fig. 5.

Potential synaptic sites demonstrated by immunocytochemistry in a day 9 co-culture. Co-immunostaining of synaptophysin and MAP2. The pre-synaptic protein synaptophysin is present at points of contact spots between the dendrites of the motoneuron and a crossing process which are usually from a sensory neuron (arrows).

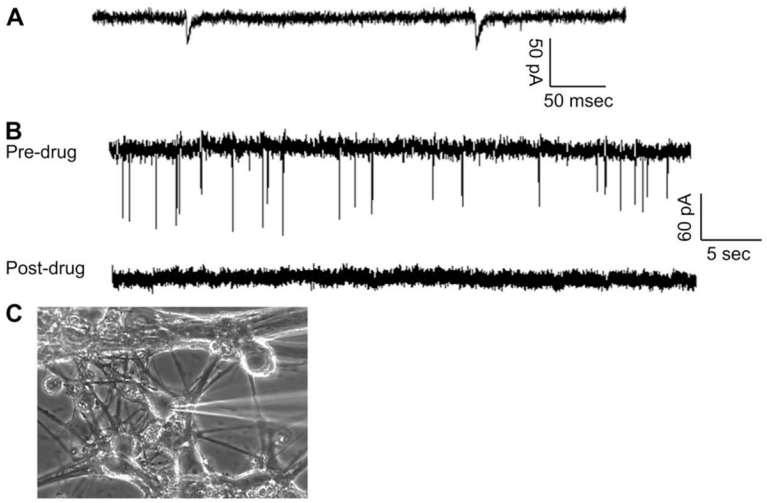

Fig. 6.

Demonstration of the synaptic connection between DRG and embryonic motoneurons. (A) An example of spontaneous mEPSCs analysis recorded from a motoneuron in close proximity to a Type Ia sensory neuron. (B) An example mEPSC recording from a motoneuron before and after the application of CNQX and 5-AP. Abundant mEPSCs were initially recorded from the motoneuron. Drug application blocked all the spontaneous activities. (C) A picture of the recorded neuron.

Table 1

Composition of enriched co-culture media.

Component	Full name	Concentration	Catalog #	Source
Neurobasal			10888	Gibco/invitrogen
B27 (50×)		1×	17504-044	Gibco/invitrogen
Glutamax (100×)		1×	35,050	Gibco/invitrogen
GDNF	Glial-derived neurotrophic factor	15 ng/ml	CRG400B	Cell sciences
BDNF	Brain-derived neurotrophic factor	20 ng/ml	CRB600B	Cell sciences
Shh	Sonic hedgehog, N-terminal peptide	50 ng/ml	1845-SH-025	R&D
RA	Retinoic acid	0.05 μM	R2625	Sigma
IGF-1	Insulin-like growth factor-I	10 ng/ml	100-11	PeproTech
cAMP	Adenosine 3,5-cyclic monophosphate	0.5 μM	A9501	Sigma
CNTF	Ciliary neurotrophic factor	22.5 ng/ml	CRC400A	Cell sciences
NT-3	Neurotrophin-3	20 ng/ml	CRN500B	Cell sciences
NT-4	Neurotrophin-4	20 ng/ml	CRN501B	Cell sciences
Vitronectin		50 ng/ml	V8379	Sigma
Vitronectin (rat plasma)		50 ng/ml	V0132	Sigma
CT-1	Cardiotrophin-1	10 ng/ml	CRC 700B	Cell sciences
LIF	Leukemia inhibitory factor	10 ng/ml	L5158	Sigma
Heparin sulfate		50 ng/ml	D9809	Sigma
Acidic FGF	Acidic Fibroblast Growth Factor	12.5 ng/ml	13241-013	Gibco/invitrogen
VEGF	Vascular Endothelial Growth Factor	10 ng/ml	P2654	Gibco/invitrogen
G5 supplement (100×)		0.5×	17503-012	Gibco/invitrogen
Antibiotic–antimycotic		0.5×	15240-062	Gibco/invitrogen
rhβ-NGF	Nerve Growth Factor	10 ng/ml	256-GF	R&D

Table 2

Electrophysiological properties of motoneurons and Type Ia sensory neurons in the co-culture.

	Membrane resistance (MΩ)	Membrane capacitance (pF)	Membrane potential (mV)	I_{Na+} (pA)	I_{K+} (pA)	AP amplitude (mV)	Repetitive AP number
DRG	294.38 ± 99.89	24.42 ± 10.34	−34.63 ± 11.92	−2799.73 ± 792.50	2144.04 ± 1508.24	113.79 ± 10.26	5.88 ± 4.26
eMN	679.94 ± 435.31	19.67 ± 9.79	−32.74 ± 17.73	−1456.93 ± 1042.32	975.73 ± 378.07	94.80 ± 14.96	7.89 ± 6.29